INFECTION AND IMMUNITY, Dec. 2007, p. 5669–5677 Vol. 75, No. 12
0019-9567/07/$08.00+0 doi:10.1128/IAI.01096-07

Chlamydia trachomatis Species-Specific Induction of Ezrin Tyrosine Phosphorylation Functions in Pathogen Entry▽

Kena A. Swanson, Deborah D. Crane, and Harlan D. Caldwell*

Laboratory of Intracellular Parasites, Rocky Mountain Laboratories, National Institute of Allergy and Infectious Diseases, National Institutes of Health, Hamilton, Montana 58940

Received 7 August 2007/Returned for modification 11 September 2007/Accepted 18 September 2007

Chlamydia trachomatis **is an obligate intracellular pathogen of humans that exhibits species-specific biological characteristics in its early interactions with host cells that are likely important to pathogenesis. One such characteristic is the tyrosine phosphorylation (Tyr-P) of an ~70-kDa polypeptide that occurs only after infection of mammalian cells by human strains. We sought to identify this protein because of its potential significance to the pathogenesis of human chlamydial infections. Using an immunoproteomic approach we identified the host protein ezrin, a member of the ezrin-radixin-moesin (ERM) protein family that serves as a physical link between host cell receptors and the actin cytoskeleton. Confocal microscopy studies showed colocalization of ezrin and actin at the tips and crypts of microvilli, the site of chlamydial attachment and entry, respectively. To demonstrate a functional role for ezrin we infected cells with a dominant-negative (DN) ezrin phenotype or treated cells with ezrin-specific small interfering RNA (siRNA). We found that both DN and siRNA-treated cells were significantly less susceptible to infection by human chlamydial strains. Moreover, we demonstrated that inhibition of infection in ezrin DN cells occurred at the stage of chlamydial entry. We hypothesize that the *C. trachomatis*-specific Tyr-P of ezrin might relate to an undefined species-specific mechanism of pathogen entry that involves chlamydial specific ligand(s) and host cell coreceptor usage.**

Chlamydiae are obligate intracellular prokaryotes that, despite a considerable degree of shared developmental biology and genomic identity, exhibit distinct host infection tropisms and clinical expression of disease (32, 33, 39). This interesting spectrum in pathogen characteristics is frequently correlated with subtle differences in in vitro infection properties, particularly treatments that affect early chlamydial infection events of cultured mammalian cells (30). Chlamydiae have a biphasic developmental cycle whereby the infectious elementary body (EB) enters the host cell, evades lysosomal fusion, and differentiates into the replicating reticulate body (RB) within a host-derived vacuole (29). Infection of cells by EBs requires both attachment and entry steps. Initial attachment is temperature independent and heparin reversible. These mechanistic properties are shared by most chlamydial strains (48), suggesting a shared common chlamydial ligand and host receptor interaction. Work with chemically mutagenized Chinese hamster ovary (CHO) cells has shown that EB entry is phenotypically distinguishable from attachment since it is temperature dependent and irreversible, and the ligands and/or receptors appear to differ among chlamydial strains (7, 18). Numerous chlamydial ligands (40, 42, 47, 48) and several host receptors (10, 15) have been implicated in attachment, leaving the precise molecular mechanisms largely unresolved and controversial. Despite the apparent species specificity governing chlamydial entry mechanisms, all chlamydiae induce the reorganization and recruitment of actin that is necessary for the entry process (6, 8).

The utilization of specific receptors by different chlamydial strains during EB entry is paralleled by observations that chlamydial entry also induces strain-specific tyrosine phosphorylation (Tyr-P) (44), suggesting a possible mechanistic relationship between these two independent observations. Previous studies have shown that entry is accompanied by the rapid Tyr-P of a number of proteins ranging in mass from 64 to 68, 97, and 140 kDa that were originally proposed to be of host cell origin (2, 16, 41). Recent reports, however, have identified an ~150-kDa protein, termed translocated actin recruiting phosphoprotein (Tarp), as being a chlamydial type III effector that is translocated to the cytoplasmic face of the host cell plasma membrane (9). Although Tyr-P is not essential for Tarp function, Tarp plays an important role in actin recruitment at the entry site (8). We recently showed that the entry-mediated Tyr-P of a 70-kDa complex of proteins was chlamydial strain dependent where infection by human *C. trachomatis* strains, but not the guinea pig pathogen *C. caviae*, induced strong Tyr-P of this complex (44). The specific induction of these Tyr-P proteins by human strains suggested to us that they might be critical in the pathogenesis of human infection.

The present study examined the 70-kDa protein complex and identified the host protein ezrin, a member of the ezrin-radixin-moesin (ERM) family that serves as a physical link between the host actin cytoskeleton and the plasma membrane. Here we show that ezrin is recruited to microvillus-like structures at sites of chlamydial entry. Importantly, ezrin is Tyr-P only upon *C. trachomatis* infection and plays an essential role in pathogen entry. This is the first confirmed identification of a host protein that is Tyr-P during chlamydial infection that is an integral component in the pathogenesis of *C. trachomatis*.

* Corresponding author. Mailing address: Laboratory of Intracellular Parasites, Rocky Mountain Laboratories, National Institute of Allergy and Infectious Diseases, National Institutes of Health, 903 S. 4th St., Hamilton, MT 59840. Phone: (406) 363-9272. Fax: (406) 363-9380. E-mail: hcaldwell@niaid.nih.gov.

▽ Published ahead of print on 1 October 2007.

MATERIALS AND METHODS

Bacterial and cell cultures. The following chlamydial strains were used: *C. trachomatis* serovars L2 (434/BU) and D (UW-3/CX) and *C. caviae* (GPIC [for guinea pig inclusion conjunctivitis]). HeLa 229 cells (ATCC CCL-2.1) were grown in modified Dulbecco's modification of Eagle's medium containing 10% fetal bovine serum, 2 mM L-glutamine, 1 mM HEPES, 1 mM sodium pyruvate, 0.055 mM β-mercaptoethanol, and 10 μg/ml gentamicin (MDMEM-10). Transfected LLC-PK1 cells, a porcine kidney epithelial cell line, were kindly provided by Monique Arpin of the Institut Curie (Paris, France). As previously described (12), LLC-PK1 cells were transfected with either the pcB6 control vector (control cells) or the vector with the N terminus of human ezrin containing a vesicular stomatitis virus G (VSVG) protein tag (dominant-negative [DN] cells). Cells remained under selection by the addition of 0.7 mg of G418/ml to the growth media. Chlamydial infections were performed by rocking at either 4°C (44) or room temperature at various multiplicities of infection (MOIs). Cells were washed twice with Hanks balanced salt solution (HBSS; Invitrogen, Carlsbad, CA) and cultured in prewarmed MDMEM-10 at 37°C and 5% CO_2. This temperature shift was designated time zero for kinetics studies. A one-step growth curve to measure recoverable inclusion-forming units was performed as described previously (5).

Abs. The anti-phosphotyrosine monoclonal antibody (Ab) 4G10 (Upstate, Charlottesville, VA), rabbit anti-actin (Bethyl Laboratories, Montgomery, TX), rabbit anti-ezrin, rabbit anti-phosphoERM, and horseradish peroxidase-conjugated anti-mouse or anti-rabbit secondary Abs (Cell Signaling Technology, Danvers, MA) were used for Western blotting. The following secondary Abs were used in microscopy studies: goat anti-mouse Cy5-, Alexa 488-, and Alexa 568-conjugated goat anti-mouse and anti-rabbit immunoglobulin G (Invitrogen). Additional Abs used were the *C. trachomatis*-specific anti-mouse L2I-10 major outer membrane protein (MOMP) Ab, anti-rabbit GPIC MOMP, fluorescein isothiocyanate-conjugated or unconjugated mouse anti-lipopolysaccharide (LPS) (EVI-H1), and mouse anti-VSVG (clone P5D4; US Biologicals, Swampscott, MA). F-actin was visualized by using Alexa 488-conjugated phalloidin (Invitrogen).

TEM. HeLa cells infected with *C. trachomatis* were fixed at the indicated times postinfection (p.i.) and processed for transmission electron microscopy (TEM) as previously described (1).

Anti-phosphotyrosine immunoaffinity purification and two-dimensional (2D) gel electrophoresis. Cells were infected at 4°C with *C. trachomatis* D (MOI of ~1,000) in T150 flasks. One hour after a temperature shift to 37°C, the cells were washed with ice-cold HBSS and scraped into cold radioimmunoprecipitation assay (RIPA) lysis buffer (1:10 dilution of 10× RIPA stock; Upstate) containing 1 mM sodium fluoride, 1 mM sodium orthovanadate (Sigma-Aldrich, St. Louis, MO), and protease inhibitor cocktail (Roche Diagnostics Corp., Indianapolis, IN). Proteins were purified by using a 4G10 immunoaffinity purification kit (Upstate) according to the manufacturer's protocol. Purified proteins were filtered through a CENTRI-SEP column and prepared for 2D analysis using a 2D Clean-Up kit according to the manufacturer's protocol (Amersham Biosciences, Piscataway, NJ). Prepared samples were separated by 2D gel electrophoresis on pI4-7 IPGphor strips (Amersham). The second dimension was separated on a 10% sodium dodecyl sulfate-polyacrylamide gel electrophoresis (SDS-PAGE) Criterion gel (Bio-Rad Laboratories, Hercules, CA). The gel was stained with Biosafe Coomassie blue G-250 (Pierce, Rockford, IL), and visualized proteins were excised. Proteins were analyzed by the Scripps Center for Mass Spectrometry (La Jolla, CA). The tandem mass spectrometry (MS/MS) analysis was performed on an LTQ mass spectrometer (Thermo Scientific, Waltham, MA). More than 15,000 MS/MS spectra were obtained during the run. These were searched by using MASCOT (v.2.1.04; Matrix Science, London, United Kingdom). Only peptides producing good quality fragmentation spectra and scoring higher than the threshold required for 95% confidence level for MASCOT were used for protein identification.

Western blotting and ezrin immunoprecipitation (IP). For kinetics of overall Tyr-P HeLa cells infected with *C. trachomatis* D (MOI of ~50) were harvested at the indicated times p.i. in cold RIPA buffer, and immunoblotting was performed as previously described (44) with the 4G10 Ab. The data shown are representative of more than four experiments. A similar procedure was used for assessing ezrin Thr-P with the anti-phosphoERM Ab except that cells were infected with *C. trachomatis* (D or L2) or GPIC (MOI of ~0.5) and harvested in Laemmli sample buffer. The phosphoERM blots were stripped and reprobed with a rabbit anti-ezrin Ab.

For ezrin IP studies, HeLa cells were infected (MOI of ~5) at 4°C in six-well tissue culture plates with either *C. trachomatis* (D or L2), GPIC, or uninfected. At the indicated times p.i., plates were placed on ice, the monolayers were washed, and cells were scraped into ice-cold HBSS. Cells were pelleted and stored at −80°C. Frozen pellets were resuspended in ice-cold RIPA buffer. Equal volumes of cleared lysates were incubated overnight at 4°C with the rabbit anti-ezrin Ab or normal rabbit serum for a negative control. The immunocomplexes were then incubated with protein A-agarose beads (Upstate), the Ab-bound beads were washed three times with cold RIPA buffer, and purified proteins were eluted by addition of 2× Laemmli buffer and a 5-min incubation at 100°C. Samples were immunoblotted with the 4G10 Ab, followed by stripping and reprobing for ezrin to show similar ezrin protein levels among samples or the absence of ezrin in the negative control IPs. The negative control IPs resulted in no purified ezrin or Tyr-P (data not shown). The data shown are representative of three or more experiments.

Confocal microscopy. To examine the cellular localization of ezrin after infection, HeLa cells were infected with *C. trachomatis* D or GPIC (MOI of ~10). At 5 and 30 min p.i., the cells were washed three times with HBSS containing heparin to remove bound nonviable bacteria. Infections lasting 4 h received the heparin wash 15 min p.i., after which the cells were cultured in MDMEM-10 for the remaining culture period. The cells were fixed by the addition of 2.5% paraformaldehyde, and coverslips were stained by indirect immunofluorescence with ezrin and chlamydial LPS-specific Abs, followed by the addition of Alexa 568- or Alexa 647-conjugated secondary Abs or Alexa 488-conjugated phalloidin to visualize F-actin. The images are representative of at least two independent experiments. All images were processed by using ImageJ (National Institutes of Health, Bethesda, MD) and Canvas software (ACD Systems, Miami, FL).

Chlamydial entry assays were performed with LLC-PK1 cells by infecting both control and DN cells on glass coverslips with either *C. trachomatis* D or GPIC (MOI of ~0.01). At 2 h p.i., cells were washed and fixed with 2.5% paraformaldehyde. Extracellular bacteria were labeled with an anti-MOMP Ab, followed by an Alexa 594-conjugated secondary Ab. Cells were then permeabilized by incubation with 0.1% saponin, followed by the addition of fluorescein isothiocyanate-conjugated anti-LPS Ab to label total bacteria. DN cells were also labeled with the anti-VSVG Ab, followed by a Cy5-conjugated secondary Ab in order to identify cells expressing the DN ezrin construct. Coverslips were mounted by using mowiol and viewed with a modified Perkin-Elmer UltraView spinning disk confocal system connected to a Nikon Eclipse TE2000-S microscope with a 60× Plan-Apo (Nikon NA 1.4) oil immersion objective lens. Images were acquired by using Metamorph software (Molecular Devices, Sunnyvale, CA). Intracellular bacteria (green only) were counted on duplicate coverslips, and the number of intracellular bacteria per cell reported in three categories: 1 to 5, 6 to 10, and 11 to 20. The results are an average of two separate experiments wherein a minimum of 20 cells per coverslip were analyzed.

Chlamydial infections of DN LLC-PK1 cells or small interfering RNA (siRNA)-treated HeLa cells. In DN experiments LLC-PK1 cells (control or DN) were infected with *C. trachomatis* (D or L2) or GPIC (MOI of ~0.01). Cells were methanol fixed 24 h p.i. and stained with anti-LPS, followed by an Alexa 488-conjugated secondary Ab. Inclusions per field were counted in triplicate, and data were normalized to infected control cells. The results are a combined average of four independent experiments. The Student *t* test was used for statistical analyses.

For siRNA knockdown studies, HeLa cells were plated at 7×10^4 cells per well in 24-well plates. The ezrin and negative control scrambled ezrin siRNA duplexes used were described by Pust et al. (31) and made by Dharmacon, Inc. (Lafayette, CO). HeLa cells were transfected with a 10 nM concentration of the individual siRNA duplexes in serum-free MDMEM using siLentFect lipid transfection reagent (Bio-Rad) according to the manufacturer's protocol (mock-transfected cells received serum-free MDMEM with transfection reagent alone). At 48 h posttransfection, the time of optimal ezrin knockdown (~40% as quantified by using densitometry of ezrin Western blots normalized to actin levels), HeLa cells were infected with *C. trachomatis* (D or L2) or GPIC (MOI of ~0.01). Cells were methanol fixed at 24 h p.i. and stained with the anti-LPS antibody, followed by an Alexa 488-conjugated secondary Ab. Inclusions per field were counted, and the results are shown as the percentage of mock-transfected cells. The data shown are representative of three independent experiments.

RESULTS

Purification and identification of tyrosine phosphorylated (Tyr-P) proteins after *C. trachomatis* infection of HeLa 229 cells. Our previous report describing Tyr-P of a 70-kDa complex of proteins showed that phosphorylation occurs rapidly upon infection and is sustained up to at least 8 h p.i (44). We

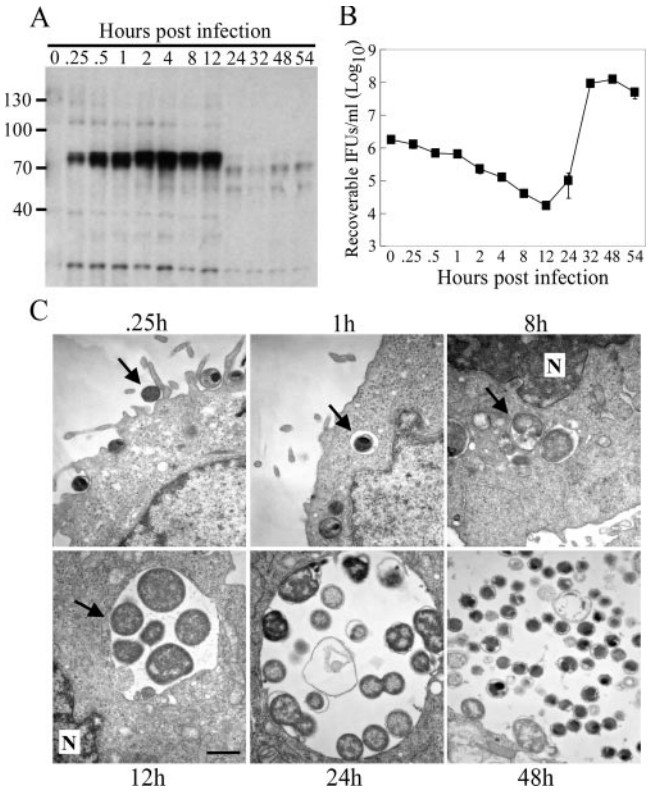

FIG. 1. The presence of Tyr-P correlates with the chlamydial developmental cycle. HeLa cells were infected with *C. trachomatis* D (MOI of ~50). (A) Western blot analysis was performed on samples at the indicated times p.i. to examine phosphotyrosine levels using the 4G10 Ab. (B) Duplicate samples were harvested, and infectious chlamydiae were quantified by replating them on new HeLa cell monolayers. Infected cells were fixed 24 h p.i. and stained with an anti-LPS Ab, and inclusions were counted in triplicate wells. Error bars indicate the standard deviation. (C) HeLa cells were infected (MOI of ~1) and fixed at the indicated times p.i. Coverslips were processed for TEM as described in Materials and Methods. Arrows in each image indicate the chlamydial EB at the early entry steps and subsequent trafficking of the early inclusion to the perinuclear region. Scale bar, 1 μm. N, nucleus.

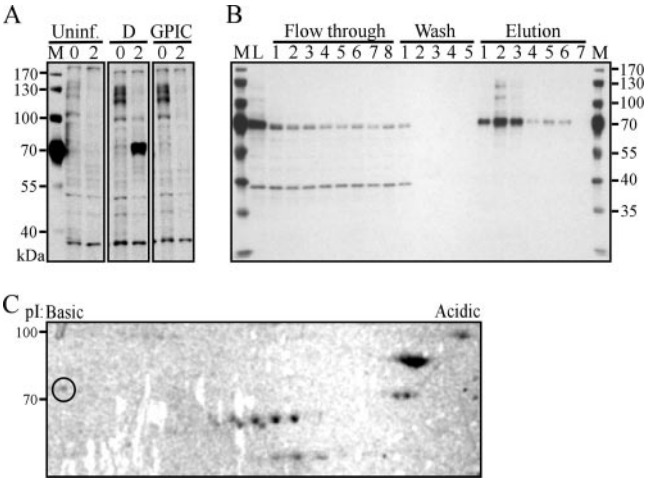

FIG. 2. Identification of ezrin as a host Tyr-P protein after *C. trachomatis* infection. (A) HeLa cells were infected with *C. trachomatis* D or GPIC (MOI of ~1) or uninfected. Cells were harvested at 0 and 2 h p.i., and cleared lysates were separated by SDS-PAGE and immunoblotted with the 4G10 Ab. M, marker. (B) Tyr-P proteins were purified from *C. trachomatis* D-infected HeLa cells (MOI of ~100) by 4G10 immunoaffinity chromatography. Purification efficiency is shown by 4G10 immunoblotting of equal volumes of collected fractions. M, marker; L, lysate. (C) Purified proteins were separated by 2D gel electrophoresis, followed by Coomassie blue staining. The circled protein spot indicates the ezrin protein identified by liquid chromatography-MS/MS.

wanted to extend these findings and determine the full kinetics of Tyr-P and how it may correlate with the chlamydial developmental cycle. Immunoblots were performed using the 4G10 anti-phosphotyrosine Ab on *C. trachomatis* serovar D-infected cell lysates obtained over the course of infection. We show that Tyr-P is most intense during the early stages of infection and is sustained up to 12 h p.i., after which it is essentially absent (Fig. 1A). As shown by the recoverable infectious organisms and electron micrographs (Fig. 1B and C), Tyr-P was present during the initial entry step of infection and maintained during the process of inclusion trafficking to the perinuclear region, at which point RBs begin to rapidly divide (21). The loss of Tyr-P occurs upon initiation of the redifferentiation process, where the noninfectious RBs transition into their infectious EB form, a point at which essential growth functions have ceased. These data suggest that Tyr-P most likely plays a role in the early phases of the chlamydial developmental cycle. The significance of this is unknown.

Tyr-P of the 70-kDa protein complex was strictly observed after *C. trachomatis* infection as shown by immunoblotting with the 4G10 Ab (Fig. 2A). In contrast, similar to uninfected cells, infection with *C. caviae* strain GPIC resulted in no measurable Tyr-P, a finding consistent with our previous report (44). To identify the proteins within the 70-kDa complex, we used immunoaffinity column chromatography with the 4G10 Ab to purify these Tyr-P proteins from *C. trachomatis* D-infected HeLa cells. Fractions were separated by SDS-PAGE and immunoblotted with the 4G10 Ab (Fig. 2B). Efficient binding to the column is indicated by the significant reduction in the 70-kDa complex after the first passage of the cell lysate over the column (L, lysate versus flowthrough, lane 1). As seen in more concentrated samples (Fig. 2B, elution 2), we observed the ~100-kDa and 130-kDa Tyr-P proteins in addition to the 70-kDa protein complex as reported by Birkelund et al. and Fawaz et al. (3, 16). 2D gel electrophoresis of the purified proteins, followed by Coomassie blue staining, showed several proteins with isoelectric points (pI) 4 to 7. Visible proteins were excised and analyzed by liquid chromatography-MS/MS (Fig. 2C).

Identified proteins included those functioning as molecular chaperones and proteins that are upregulated during cell stress, such as the heat shock proteins HSP60, HSP70, and HSP90 (Table 1). More interestingly, ezrin, a protein that associates with host cell membrane receptors and the actin cytoskeleton, was also identified (Fig. 2C, circled spot). Coomassie blue staining indicated that ezrin was not the most abundant protein, which could contribute to the lower number of matched peptides from the MS analysis. Ezrin has a theoretical molecular mass of 69 kDa and a pI of 5.94 (19). In our study, ezrin migrated to ~85 kDa and showed an empirical pI

TABLE 1. Anti-phosphotyrosine immunoaffinity-purified proteins from *C. trachomatis*-infected HeLa 229 cells

Spot	Protein	Matched peptide(s)	Molecular mass (kDa)[a]		pI		Accession no.[b]
			Predicted	Pre-ID	Predicted	Pre-ID	
1	Endoplasmin precursor (GRP 94)	11	92	130	4.76	4.8	P14625
2	HSP90 alpha/HSP90 beta	16/9	85/83	100	4.94/4.97	5	P07900/P08238
3	78-kDa glucose regulated protein precursor (GRP 78)	15	72	72	5.07	5.1	P11021
4	Ezrin	2	69	85	5.94	6.5	CAI95307
5	Heat shock cognate 71-kDa protein	8	71	68	5.37	5.6	P11142
6	HSP60	7	60	60	5.7	5.5	P10809
7	T-complex protein 1 gamma subunit (TCP-1)	2	57	60	6.01	6.3	P49368

[a] The predicted values are from the Swiss-Prot database accessed through the ProtParam tool on the ExPASy proteomics server. The pre-identification (pre-ID) values were estimated based on empirical isoelectric focusing and protein mobility using 2D gel electrophoresis.
[b] Accession numbers are according to the NCBI nomenclature.

of ~6.5. Our results are in accordance with previous reports that describe ezrin migration to ~80 kDa and a more basic pI of 6.15 (4).

Species-specific ezrin Tyr-P. Ezrin activation involves phosphorylation of a conserved C-terminal threonine residue (Thr567) (17), which disrupts the inhibitory intramolecular interaction between its N and C termini, permitting the interaction of these domains with membrane proteins (e.g., host cell receptors) and F-actin, respectively (43). Subsequent Tyr-P, in addition to stabilizing the active form, is also important for the induction of intracellular signaling cascades initiated after host-pathogen interactions (36). Upon examination of the ezrin activation status after infection, we found that threonine phosphorylation (Thr-P) is ubiquitous among the chlamydial strains tested, as shown by immunoblotting with a phosphoERM Ab specific to the conserved C-terminal Thr (Fig. 3A). Quantitation of phosphoERM levels by densitometry showed that the induction of ezrin Thr-P was specific to infected cells (Fig. 3B). A significant induction of ezrin Thr-P after infection was seen at the early time points p.i. Thereafter (~4 h p.i.), similar levels of ezrin Thr-P were observed between infected and uninfected cells.

To assess Tyr-P, ezrin was immunoprecipitated, followed by immunoblotting with the 4G10 Ab. These experiments showed that ezrin Tyr-P is specific to *C. trachomatis*-infected cells and, consistent with the characterized ezrin activation mechanisms, Tyr-P appears to be subsequent to Thr-P (Fig. 3C). Furthermore, in contrast to Thr-P of ezrin, Tyr-P is more specific to infection since Tyr-P was absent from uninfected cells throughout the culture period. This suggests that a highly specific pathogen-derived trigger is responsible for the additional ezrin activation through Tyr-P. Interestingly, the previously reported subtle molecular mass difference in the Tyr-P proteins within the 70-kDa complex between trachoma and lymphogranuloma venereum *C. trachomatis* strains (44) was further highlighted upon examination of ezrin Tyr-P (Fig. 3C, arrowheads). Together, these data suggest that species-common and species-specific entry pathways exist, leading to ezrin Thr567 and/or Tyr-P, respectively.

Ezrin localization during chlamydial infection. The entry of multiple pathogens involves the recruitment of host proteins to the site of attachment to facilitate actin recruitment. Because of our evidence of ezrin Tyr-P early in infection, we expected to see ezrin recruitment along with actin filaments to sites of EB attachment. To examine this, HeLa cells were infected with *C. trachomatis* D, fixed, and processed for indirect immunofluorescence at 5 min, 30 min, and 4 h p.i. EBs were observed in microvillus-like structures wherein ezrin and actin were localized at 5 min p.i. (Fig. 4A). Under steady-state conditions ezrin is primarily localized in the cytoplasm; however, upon activation it is recruited to the plasma membrane and binds F-actin to aid in microvillus formation. Accordingly, ezrin was essentially absent in the host cell cytosol and was primarily observed in microvillus-like structures. Uninfected cells also displayed ezrin-rich microvillus structures; however, they were much less abundant in comparison to infected cells (data not shown). Consistent with the species-common induction of ezrin Thr-P during infection, ezrin was also similarly recruited to cells infected with GPIC (data not shown). This suggests that there are species-specific signaling pathways induced during *C. trachomatis* invasion leading to ezrin phosphorylation on tyrosine residues. Ultrastructural studies have shown that EBs initially bind the tips of microvilli and then transfer to the crypts, or base, of these cell projections (11, 24). We observed similar localization of *C. trachomatis* D EBs on microvilli, where ezrin was found concentrated around the EBs and along the microvillus-like structure (Fig. 4A and B).

Ezrin Tyr-P is sustained up to 12 h p.i. with *C. trachomatis* D (Fig. 2). Examination of ezrin localization postentry (4 h p.i.) showed a predominant cytosolic distribution, with punctate structures localized near trafficking early inclusions (Fig. 4C). Similar ezrin localization was observed at 12 h p.i.; however, at 24 h p.i. no significant ezrin association was observed with the chlamydial inclusion (data not shown). This localization suggests that ezrin may also be involved in postentry events during *C. trachomatis* development.

Ezrin functions in *C. trachomatis* EB entry. We have shown ezrin recruitment to microvillus-like structures during chlamydial entry. To assess the functional importance of ezrin in the chlamydial entry step, we quantified the entry efficiency of *C. trachomatis* EBs. Specifically, ezrin DN or control LLC-PK1 cells (expressing the empty vector) were infected with *C. trachomatis* D or GPIC for 2 h, after which the cells were fixed and stained to differentiate between extracellular and internalized EBs. Compared to control cells, *C. trachomatis*-infected DN cells showed a marked reduction in the number of internalized EBs per cell (Fig. 5). The majority of infected cells contained between one and five EBs, and only a fraction of the

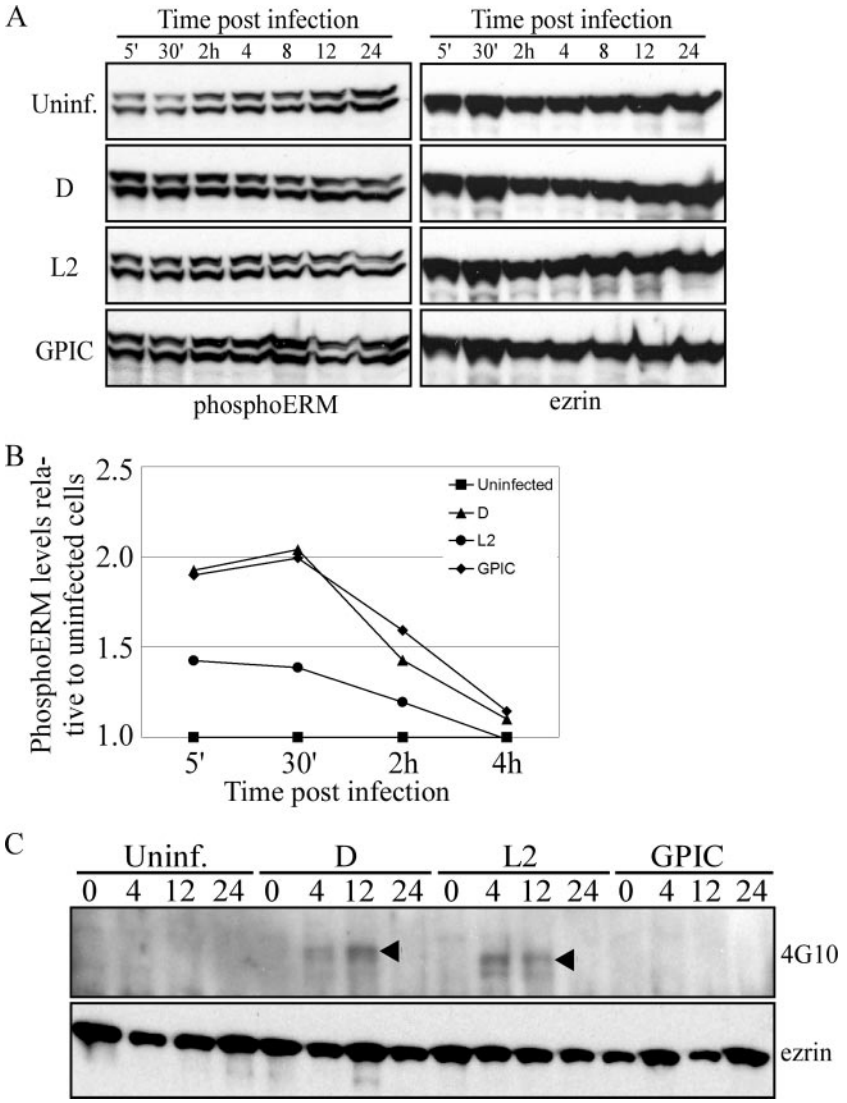

FIG. 3. *C. trachomatis*-specific ezrin Tyr-P is sustained to the mid-cycle of infection. (A) Ezrin Thr-P occurs independently of the infecting chlamydial strain. Cells remained uninfected or were infected with either *C. trachomatis* (D or L2) or GPIC (MOI of ~0.5). Samples were harvested at the indicated times p.i. in Laemmli sample buffer, and Thr-P was determined by immunoblotting with an anti-phosphoERM Ab specific to the C-terminal Thr567. The same blots were stripped and reprobed for total ezrin. (B) Densitometry was performed on the blots shown in panel A. PhosphoERM levels were normalized to total ezrin levels within each sample. The graph shows the fold change in phosphoERM levels relative to uninfected cells, with values from uninfected cells set to 1. (C) Cells were infected as described above (MOI of ~5), and ezrin was immunoprecipitated with an anti-rabbit ezrin Ab. The Tyr-P status was examined by Western blotting with the 4G10 Ab. The same blot was stripped and reprobed with the anti-ezrin Ab.

infected cells contained six to ten EBs per cell. Upon infection with GPIC, no observable difference in internalized EBs occurred between control and DN cells.

Ezrin-dependent *C. trachomatis* infection. LLC-PK1 cells were used to further assess the functional significance of ezrin during *C. trachomatis* infection. DN and control cells were infected with either *C. trachomatis* (D or L2) or GPIC. Infected cells were fixed 24 h p.i., and inclusions were quantified by indirect immunofluorescence using an anti-LPS Ab to determine infection efficiency. Infection of DN cells with *C. trachomatis* resulted in a significant decrease in chlamydial inclusions (Fig. 6A). In contrast, no reduction in infectivity was observed with GPIC.

In addition to DN cells, we also used siRNA to knock down the ezrin message in HeLa cells prior to infection. Transfection of ezrin-specific siRNA duplexes consistently resulted in ca. 40% reduction in protein levels as determined by densitometry of ezrin immunoblots (Fig. 6B). Two rounds of siRNA transfection, as well as a pool of ezrin-specific siRNAs, did not improve ezrin protein knockdown (data not shown). Ezrin is a constitutively expressed and highly stable protein that could explain the less efficient reduction in ezrin protein levels. As shown in Fig. 6C, there was a significant reduction in *C. trachomatis* infectivity but not of GPIC. Furthermore, cells that received scrambled ezrin siRNA showed no significant reduction in infection efficiency with all strains (Fig. 6D).

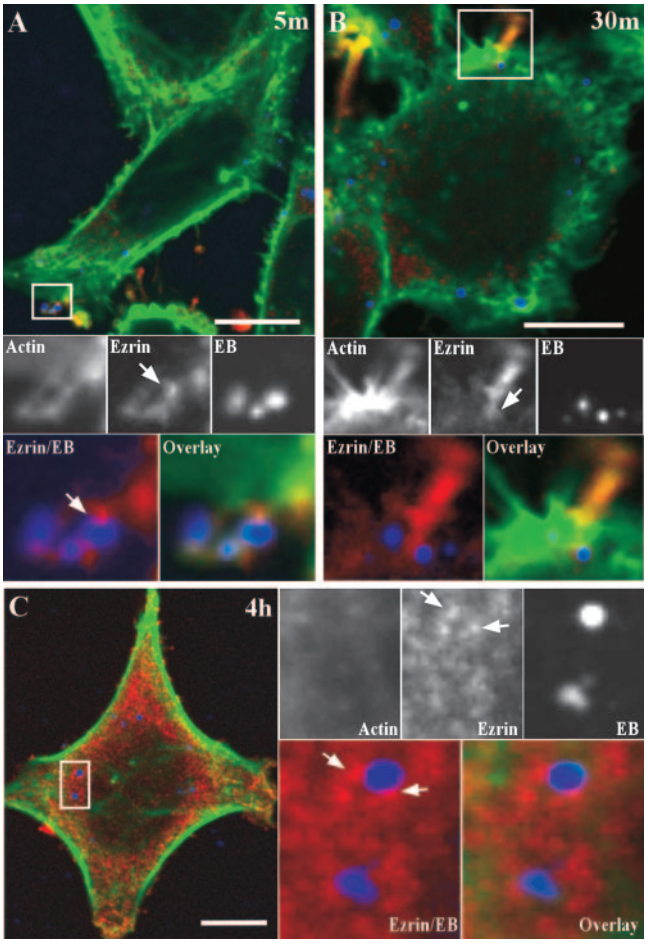

FIG. 4. Ezrin recruitment to the EB entry site and early chlamydial inclusion. HeLa cells were infected with *C. trachomatis* D (MOI of ~1). At 5 min (A) and 30 min (B) the cells were fixed and triple labeled by indirect immunofluorescence with anti-ezrin (red), anti-LPS (blue), and Alexa 488-conjugated phalloidin (green) for labeling of F-actin. (A) Confocal microscopy image showing ezrin and actin recruited to the tips of microvillus-like structures where three EBs are attached. The arrow indicates the ezrin-EB localization. Scale bar, 10 μm. (B) At 30 min p.i., ezrin is still seen associated with EBs during the entry process. The arrow indicates ezrin localization with EB in the crypt of the microvillus-like structure. Scale bar, 10 μm. (C) Ezrin localizes with early trafficking inclusions. HeLa cells were treated as in panels A and B except that the cells were fixed at 4 h p.i. Two trafficking early inclusions containing individual EBs are shown where ezrin is closely localized. Arrows indicate the punctate ezrin localization with the early inclusion. Scale bar, 2 μm.

DISCUSSION

Here we show for the first time that *C. trachomatis* infection induces Tyr-P of the host protein ezrin in a species-specific manner. Ezrin was not Tyr-P after infection with *C. caviae* GPIC, a pathogen of guinea pigs with no known human zoonosis. We also demonstrate a functional role for ezrin in *C. trachomatis* entry by using ezrin DN and siRNA-treated cells. The absence of complete inhibition of *C. trachomatis* EB entry suggests that chlamydiae are able to use additional ezrin-independent mechanisms for entry into host cells. Consistent with this, recent reports have described multiple entry mechanisms used by *C. trachomatis* (14, 25). Interestingly, ezrin Thr-P occurred in a species-independent manner, suggesting that initial ezrin activation is ubiquitous among chlamydiae; however, pathways leading to ezrin Tyr-P are species dependent. A similar distinction with ezrin activation was previously described with the comparison of enterpathogenic (EPEC) and enterohemorrhagic (EHEC) *Escherichia coli*. Both EPEC and EHEC show similar pedestal formation and recruitment of ezrin (20); however, only EPEC has been shown to induce ezrin Tyr-P (36). Ezrin phosphorylation on Tyr residues is linked to signal-specific intracellular signaling cascades via its interaction with the cytoplasmic tail of a number of host cell receptors. For example, Tyr145 and Tyr353 are phosphorylated through stimulation of the epidermal growth factor receptor (26). Cross-linking of intercellular adhesion molecule 1 activates Src tyrosine kinases (45), and molecular studies have shown that Src kinase induces ezrin Tyr-P at residue 477 (23). Therefore, the Tyr residues phosphorylated upon *C. trachomatis* infection are likely linked to the activation or modification of specific host cell receptors that function in binding to EB adhesins important to chlamydial entry. This would intuitively argue that *C. trachomatis* and *C. caviae* utilize different host cell receptors for entry.

This hypothesis is supported by studies with chemically mutagenized CHO cells that exhibit different susceptibilities to infection by *C. trachomatis* and *C. pneumoniae* (18). Although we did not study *C. pneumoniae* here, we previously reported that infection with *C. pneumoniae*, like that with *C. caviae*, failed to induce Tyr-P of the 70-kDa protein that we have now identified as ezrin. In a related study, Carabeo and Hackstadt showed that *C. trachomatis* D and L2 entered cells by noncompeting independent mechanisms (7). The subtle molecular mass differences we observed in Tyr-P ezrin after infection with these biovars (Fig. 3B) implies that the mechanism of Tyr-P ezrin differs within the *C. trachomatis* species. Together, these data suggest distinct differences in the cognate receptor engaged, and likely tyrosine kinases recruited, after infection by these biovars.

What are the potential host cell receptor candidates for *C. trachomatis* infection? Ezrin is known to interact with the cytoplasmic domain of several receptors, including CD44, members of the integrin super family, and intercellular adhesion molecules; all of which have been shown to play a role in the entry process of both bacterial and viral pathogens (13, 27, 35). For example, *Shigella flexneri* has been shown to enter host cells through interaction of the type III-secreted Ipa invasins with $\alpha_5\beta_1$ integrin and CD44, which is followed by ezrin activation and recruitment (37, 38, 46). Recent studies in attachment of *C. trachomatis* suggest a role for protein disulfide isomerase (PDI), a member of the estrogen receptor complex (10, 15); however, it is unclear whether PDI serves as an actual receptor or coreceptor or perhaps simply functions enzymatically to prepare the chlamydial ligand or host cell receptor for interaction. Furthermore, there is currently no evidence showing that PDI ligation leads to ezrin Tyr-P.

We observed that ezrin closely associates with the early chlamydial inclusion (4 to 12 h p.i.), although no evidence for actin recruitment to the inclusion periphery was observed (Fig. 4C). Interestingly, this association closely paralleled the temporal kinetics of ezrin Tyr-P (Fig. 3B). Collectively, these find-

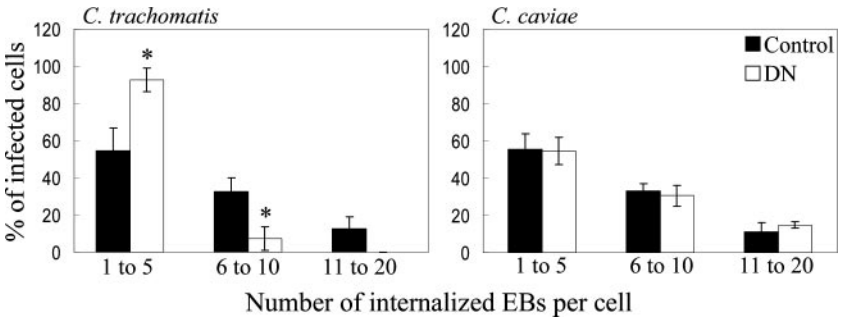

FIG. 5. Ezrin functions during *C. trachomatis* entry. Control or DN LLC-PK1 cells were infected with *C. trachomatis* D or GPIC (MOI of ~0.01). Cells were fixed at 2 h p.i., and extracellular bacteria were stained with a MOMP-specific Ab. The cells were permeabilized, and the total bacteria were stained with an LPS-specific Ab. The number of internalized EBs was quantified and categorized according to number of intracellular EBs per cell. Only with *C. trachomatis* D infection was there a significant reduction in the number of EBs per infected cell. *, $P < 0.002$.

ings implicate a secondary downstream function for ezrin Tyr-P. We hypothesize that ezrin Tyr-P may play a role in inclusion trafficking, specifically aiding in early inclusion trafficking for the purpose of singular inclusion formation. Consistent with this hypothesis is our finding that both strains that induce ezrin Tyr-P (L2 and D) are fusogenic after coinfection of epithelial cells, whereas coinfection with D and GPIC (which failed to induce ezrin Tyr-P) showed no heterotypic inclusion fusion (data not shown). These species-specific inclusion properties have been illustrated in the association of GTP-bound Rab6 with *C. trachomatis* inclusions (34). Bicaudal D1 (BICD1), a Rab6 effector, was shown to be specifically recruited to the inclusion in a chlamydial biovar-specific manner (28). There are interesting parallels between BICD1 and ezrin as both display small GTPase-dependent intermolecular interactions that confer the active state. Thus, it is tempting to speculate as to whether Rab6 may be involved in ezrin Tyr-P and the subsequent association with trafficking inclusions. Rab11 also associates with *C. trachomatis* inclusions, and the Rab11-FIP3 and Rab11-FIP4 interacting proteins contain a C-terminal ERM domain (22), further supporting a possible ezrin-RabGTPase interaction that might function in inclusion trafficking and biogenesis.

We outline here a direct role for Tyr-P ezrin in *C. trachomatis* entry and indirectly for a downstream secondary function that might affect inclusion biogenesis. This information will be an invaluable tool in our future work aimed at identifying the chlamydial EB ligand or secreted effector that mediates interaction with its cognate host cell receptor(s) utilized for pathogen entry. Defining these important virulence factors and their

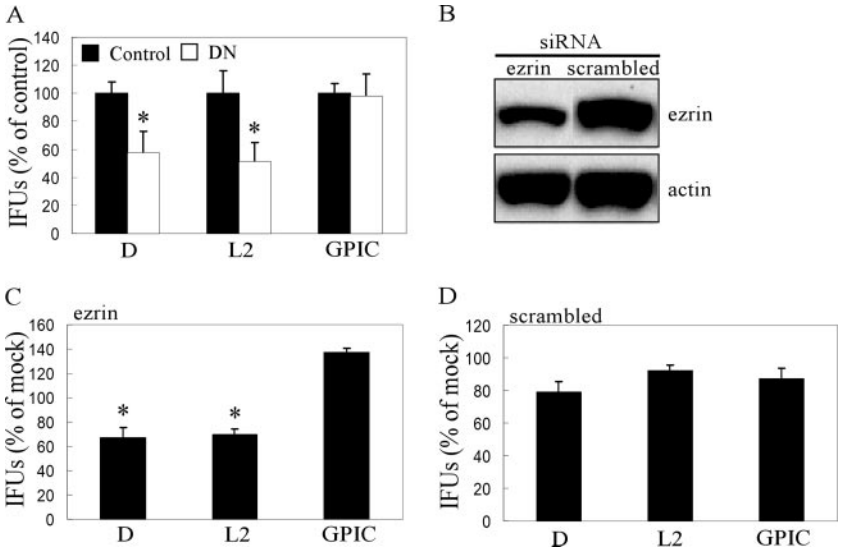

FIG. 6. Ezrin-dependent *C. trachomatis* infection. (A) LLC-PK1 cells stably expressing the DN ezrin (DN, white bars) or control vector (Control, black bars) were infected with *C. trachomatis* (D or L2) or GPIC (MOI of ~0.1). At 24 h p.i., the cells were fixed and stained with the anti-LPS Ab. Inclusions were quantified and normalized to infected control cells. In all experiments, control cells contained between approximately 200 to 300 inclusions across individual wells. Error bars indicate standard deviation. *, $P < 0.005$. (B) HeLa cells were transfected with ezrin-specific or scrambled ezrin siRNA. Ezrin protein levels were examined by Western blotting at 48 h posttransfection, the time of chlamydial infection. There was an ~40% reduction in ezrin protein levels. (C and D) HeLa cells transfected with ezrin-specific (C) or scrambled (D) siRNA were infected 48 h posttransfection with *C. trachomatis* (D or L2) or GPIC (MOI of ~0.01). Cells were fixed and stained 24 h p.i. as described above, and the inclusions were quantified. The values shown represent inclusion-forming units (IFUs) as a percentage of mock-transfected cells. *, $P < 0.001$.

host cell targets will be pivotal in the pursuit of novel strategies for the prevention and control of infection by this medically important global pathogen.

ACKNOWLEDGMENTS

We thank Robert Heinzen, Leigh Knodler, and Olivia Steele-Mortimer for critical review of the manuscript; Monique Arpin for the use of the LLC-PK1 cells; Wandy Beatty for the TEM; Sunia Trauger of the Scripps Center for the mass spectrometry; Naomi Crane for technical assistance; Bill Whitmire for chlamydial preparations; Anita Mora for graphical assistance; and Kelly Matteson for editorial assistance.

This study was supported by the Intramural Research Program of the National Institute of Allergy and Infectious Diseases, National Institutes of Health.

REFERENCES

1. **Belland, R. J., G. Zhong, D. D. Crane, D. Hogan, D. Sturdevant, J. Sharma, W. L. Beatty, and H. D. Caldwell.** 2003. Genomic transcriptional profiling of the developmental cycle of *Chlamydia trachomatis*. Proc. Natl. Acad. Sci. USA **100:**8478–8483.
2. **Birkelund, S., L. Bini, V. Pallini, M. Sanchez-Campillo, S. Liberatori, J. D. Clausen, S. Ostergaard, A. Holm, and G. Christiansen.** 1997. Characterization of *Chlamydia trachomatis* L2-induced tyrosine-phosphorylated HeLa cell proteins by two-dimensional gel electrophoresis. Electrophoresis **18:**563–567.
3. **Birkelund, S., H. Johnsen, and G. Christiansen.** 1994. *Chlamydia trachomatis* serovar L2 induces protein tyrosine phosphorylation during uptake by HeLa cells. Infect. Immun. **62:**4900–4908.
4. **Bretscher, A.** 1983. Purification of an 80,000-dalton protein that is a component of the isolated microvillus cytoskeleton, and its localization in non-muscle cells. J. Cell Biol. **97:**425–432.
5. **Caldwell, H. D., J. Kromhout, and J. Schachter.** 1981. Purification and partial characterization of the major outer membrane protein of *Chlamydia trachomatis*. Infect. Immun. **31:**1161–1176.
6. **Carabeo, R. A., S. S. Grieshaber, E. Fischer, and T. Hackstadt.** 2002. *Chlamydia trachomatis* induces remodeling of the actin cytoskeleton during attachment and entry into HeLa cells. Infect. Immun. **70:**3793–3803.
7. **Carabeo, R. A., and T. Hackstadt.** 2001. Isolation and characterization of a mutant Chinese hamster ovary cell line that is resistant to *Chlamydia trachomatis* infection at a novel step in the attachment process. Infect. Immun. **69:**5899–5904.
8. **Clifton, D. R., C. A. Dooley, S. S. Grieshaber, R. A. Carabeo, K. A. Fields, and T. Hackstadt.** 2005. Tyrosine phosphorylation of the chlamydial effector protein Tarp is species specific and not required for recruitment of actin. Infect. Immun. **73:**3860–3868.
9. **Clifton, D. R., K. A. Fields, S. S. Grieshaber, C. A. Dooley, E. R. Fischer, D. J. Mead, R. A. Carabeo, and T. Hackstadt.** 2004. A chlamydial type III translocated protein is tyrosine-phosphorylated at the site of entry and associated with recruitment of actin. Proc. Natl. Acad. Sci. USA **101:**10166–10171.
10. **Conant, C. G., and R. S. Stephens.** 2007. *Chlamydia* attachment to mammalian cells requires protein disulfide isomerase. Cell Microbiol. **9:**222–232.
11. **Coombes, B. K., and J. B. Mahony.** 2002. Identification of MEK- and phosphoinositide 3-kinase-dependent signaling as essential events during *Chlamydia pneumoniae* invasion of HEp2 cells. Cell Microbiol. **4:**447–460.
12. **Crepaldi, T., A. Gautreau, P. M. Comoglio, D. Louvard, and M. Arpin.** 1997. Ezrin is an effector of hepatocyte growth factor-mediated migration and morphogenesis in epithelial cells. J. Cell Biol. **138:**423–434.
13. **Cywes, C., and M. R. Wessels.** 2001. Group A streptococcus tissue invasion by CD44-mediated cell signaling. Nature **414:**648–652.
14. **Dautry-Varsat, A., A. Subtil, and T. Hackstadt.** 2005. Recent insights into the mechanisms of *Chlamydia* entry. Cell Microbiol. **7:**1714–1722.
15. **Davis, C. H., J. E. Raulston, and P. B. Wyrick.** 2002. Protein disulfide isomerase, a component of the estrogen receptor complex, is associated with *Chlamydia trachomatis* serovar E attached to human endometrial epithelial cells. Infect. Immun. **70:**3413–3418.
16. **Fawaz, F. S., C. van Ooij, E. Homola, S. C. Mutka, and J. N. Engel.** 1997. Infection with *Chlamydia trachomatis* alters the tyrosine phosphorylation and/or localization of several host cell proteins including cortactin. Infect. Immun. **65:**5301–5308.
17. **Fievet, B. T., A. Gautreau, C. Roy, L. Del Maestro, P. Mangeat, D. Louvard, and M. Arpin.** 2004. Phosphoinositide binding and phosphorylation act sequentially in the activation mechanism of ezrin. J. Cell Biol. **164:**653–659.
18. **Fudyk, T., L. Olinger, and R. S. Stephens.** 2002. Selection of mutant cell lines resistant to infection by *Chlamydia trachomatis* and *Chlamydia pneumoniae*. Infect. Immun. **70:**6444–6447.
19. **Gasteiger, E., A. Gattiker, C. Hoogland, I. Ivanyi, R. D. Appel, and A. Bairoch.** 2003. ExPASy: the proteomics server for in-depth protein knowledge and analysis. Nucleic Acids Res. **31:**3784–3788.
20. **Goosney, D. L., R. DeVinney, and B. B. Finlay.** 2001. Recruitment of cytoskeletal and signaling proteins to enteropathogenic and enterohemorrhagic *Escherichia coli* pedestals. Infect. Immun. **69:**3315–3322.
21. **Hackstadt, T.** 1999. Cell biology, p. 101–138. *In* R. S. Stephens (ed.), *Chlamydia*: intracellular biology, pathogenesis, and immunity. American Society for Microbiology, Washington, DC.
22. **Hales, C. M., R. Griner, K. C. Hobdy-Henderson, M. C. Dorn, D. Hardy, R. Kumar, J. Navarre, E. K. Chan, L. A. Lapierre, and J. R. Goldenring.** 2001. Identification and characterization of a family of Rab11-interacting proteins. J. Biol. Chem. **276:**39067–39075.
23. **Heiska, L., and O. Carpen.** 2005. Src phosphorylates ezrin at tyrosine 477 and induces a phospho-specific association between ezrin and a kelch-repeat protein family member. J. Biol. Chem. **280:**10244–10252.
24. **Hodinka, R. L., and P. B. Wyrick.** 1986. Ultrastructural study of mode of entry of *Chlamydia psittaci* into L-929 cells. Infect. Immun. **54:**855–863.
25. **Hybiske, K., and R. S. Stephens.** 2007. Mechanisms of *Chlamydia trachomatis* entry into nonphagocytic cells. Infect. Immun. **75:**3925–3934.
26. **Krieg, J., and T. Hunter.** 1992. Identification of the two major epidermal growth factor-induced tyrosine phosphorylation sites in the microvillar core protein ezrin. J. Biol. Chem. **267:**19258–19265.
27. **Merz, A. J., C. A. Enns, and M. So.** 1999. Type IV pili of pathogenic neisseriae elicit cortical plaque formation in epithelial cells. Mol. Microbiol. **32:**1316–1332.
28. **Moorhead, A. R., K. A. Rzomp, and M. A. Scidmore.** 2007. The Rab6 effector Bicaudal D1 associates with *Chlamydia trachomatis* inclusions in a biovar-specific manner. Infect. Immun. **75:**781–791.
29. **Moulder, J. W.** 1991. Interaction of chlamydiae and host cells in vitro. Microbiol. Rev. **55:**143–190.
30. **Moulder, J. W., T. P. Hatch, C. C. Kuo, J. Schachter, and J. Storz.** 1984. Chlamydia, p. 729–739. *In* N. R. Krieg (ed.), Bergey's manual of systematic bacteriology, vol. 1. The Williams & Wilkins Co., Baltimore, MD.
31. **Pust, S., H. Morrison, J. Wehland, A. S. Sechi, and P. Herrlich.** 2005. *Listeria monocytogenes* exploits ERM protein functions to efficiently spread from cell to cell. EMBO **24:**1287–1300.
32. **Read, T. D., R. C. Brunham, C. Shen, S. R. Gill, J. F. Heidelberg, O. White, E. K. Hickey, J. Peterson, T. Utterback, K. Berry, S. Bass, K. Linher, J. Weidman, H. Khouri, B. Craven, C. Bowman, R. Dodson, M. Gwinn, W. Nelson, R. DeBoy, J. Kolonay, G. McClarty, S. L. Salzberg, J. Eisen, and C. M. Fraser.** 2000. Genome sequences of *Chlamydia trachomatis* MoPn and *Chlamydia pneumoniae* AR39. Nucleic Acids Res. **28:**1397–1406.
33. **Read, T. D., G. S. Myers, R. C. Brunham, W. C. Nelson, I. T. Paulsen, J. Heidelberg, E. Holtzapple, H. Khouri, N. B. Federova, H. A. Carty, L. A. Umayam, D. H. Haft, J. Peterson, M. J. Beanan, O. White, S. L. Salzberg, R. C. Hsia, G. McClarty, R. G. Rank, P. M. Bavoil, and C. M. Fraser.** 2003. Genome sequence of *Chlamydophila caviae* (*Chlamydia psittaci* GPIC): examining the role of niche-specific genes in the evolution of the *Chlamydiaceae*. Nucleic Acids Res. **31:**2134–2147.
34. **Rzomp, K. A., L. D. Scholtes, B. J. Briggs, G. R. Whittaker, and M. A. Scidmore.** 2003. Rab GTPases are recruited to chlamydial inclusions in both a species-dependent and species-independent manner. Infect. Immun. **71:**5855–5870.
35. **Sharma-Walia, N., P. P. Naranatt, H. H. Krishnan, L. Zeng, and B. Chandran.** 2004. Kaposi's sarcoma-associated herpesvirus/human herpesvirus 8 envelope glycoprotein gB induces the integrin-dependent focal adhesion kinase-Src-phosphatidylinositol 3-kinase-rho GTPase signal pathways and cytoskeletal rearrangements. J. Virol. **78:**4207–4223.
36. **Simonovic, I., M. Arpin, A. Koutsouris, H. J. Falk-Krzesinski, and G. Hecht.** 2001. Enteropathogenic *Escherichia coli* activates ezrin, which participates in disruption of tight junction barrier function. Infect. Immun. **69:**5679–5688.
37. **Skoudy, A., J. Mounier, A. Aruffo, H. Ohayon, P. Gounon, P. Sansonetti, and G. Tran Van Nhieu.** 2000. CD44 binds to the Shigella IpaB protein and participates in bacterial invasion of epithelial cells. Cell Microbiol. **2:**19–33.
38. **Skoudy, A., G. T. Nhieu, N. Mantis, M. Arpin, J. Mounier, P. Gounon, and P. Sansonetti.** 1999. A functional role for ezrin during *Shigella flexneri* entry into epithelial cells. J. Cell Sci. **112**(Pt. 13)**:**2059–2068.
39. **Stephens, R. S., S. Kalman, C. Lammel, J. Fan, R. Marathe, L. Aravind, W. Mitchell, L. Olinger, R. L. Tatusov, Q. Zhao, E. V. Koonin, and R. W. Davis.** 1998. Genome sequence of an obligate intracellular pathogen of humans: *Chlamydia trachomatis*. Science **282:**754–759.
40. **Su, H., L. Raymond, D. D. Rockey, E. Fischer, T. Hackstadt, and H. D. Caldwell.** 1996. A recombinant *Chlamydia trachomatis* major outer membrane protein binds to heparan sulfate receptors on epithelial cells. Proc. Natl. Acad. Sci. USA **93:**11143–11148.
41. **Subtil, A., B. Wyplosz, M. E. Balana, and A. Dautry-Varsat.** 2004. Analysis of *Chlamydia caviae* entry sites and involvement of Cdc42 and Rac activity. J. Cell Sci. **117:**3923–3933.
42. **Ting, L. M., R. C. Hsia, C. G. Haidaris, and P. M. Bavoil.** 1995. Interaction of outer envelope proteins of *Chlamydia psittaci* GPIC with the HeLa cell surface. Infect. Immun. **63:**3600–3608.
43. **Tsukita, S., and S. Yonemura.** 1999. Cortical actin organization: lessons from ERM (ezrin/radixin/moesin) proteins. J. Biol. Chem. **274:**34507–34510.
44. **Virok, D. P., D. E. Nelson, W. M. Whitmire, D. D. Crane, M. M. Goheen, and H. D. Caldwell.** 2005. Chlamydial infection induces pathobiotype-specific protein tyrosine phosphorylation in epithelial cells. Infect. Immun. **73:**1939–1946.

45. **Wang, Q., G. R. Pfeiffer II, and W. A. Gaarde.** 2003. Activation of SRC tyrosine kinases in response to ICAM-1 ligation in pulmonary microvascular endothelial cells. J. Biol. Chem. **278:**47731–47743.
46. **Watarai, M., S. Funato, and C. Sasakawa.** 1996. Interaction of Ipa proteins of *Shigella flexneri* with alpha5beta1 integrin promotes entry of the bacteria into mammalian cells. J. Exp. Med. **183:**991–999.
47. **Wehrl, W., V. Brinkmann, P. R. Jungblut, T. F. Meyer, and A. J. Szczepek.** 2004. From the inside out–processing of the Chlamydial autotransporter PmpD and its role in bacterial adhesion and activation of human host cells. Mol. Microbiol. **51:**319–334.
48. **Zhang, J. P., and R. S. Stephens.** 1992. Mechanism of *Chlamydia trachomatis* attachment to eukaryotic host cells. Cell **69:**861–869.

Editor: R. P. Morrison